Research article

Journal of RAMAN SPECTROSCOPY

Received: 12 March 2017 Revised: 18 May 2017 Accepted: 18 May 2017 Published online in Wiley Online Library: 20 June 2017

(wileyonlinelibrary.com) DOI 10.1002/jrs.5189

Raman bands of twisted bilayer graphene

Valentin N. Popov*

A theoretical approach to the modelling of the resonant Raman scattering by phonons in twisted bilayer graphene is developed and presented. The normally very large unit cells of twisted bilayer graphene hinder the large scale calculation of the electronic, vibrational, and optical properties by microscopic models. Here, a perturbative approach within a non-orthogonal tight-binding model is proposed that allows for a significant reduction of the computational time for such calculations. This approach is applied to the electronic band structure, electronic density of states, dielectric function, and Raman excitation profile of the most intense first-order Raman band – the G band – for twisted bilayer graphene with up to a few hundred carbon atoms in the unit cell. The computational scheme can easily be extended to second-order Raman bands of twisted bilayer graphene as well. The obtained theoretical predictions can be used for characterization of twisted bilayer graphene samples, using experimental Raman data.

Keywords: theory; twisted bilayer graphene; electronic structure; dielectric function; Raman excitation profile

Introduction

Graphene is a two-dimensional honeycomb structure consisting entirely of carbon atoms. It can be considered as a building block of the naturally existing graphite with hexagonal (AB) and rhombohedral (ABC) stacking. Recently, single-layer graphene (SLG), bilayer graphene (BLG), and, more generally, few-layer graphene (FLG) have been in the focus of many experimental and theoretical works (for review, see, e.g., Novoselov *et al.*[1]). FLG, obtained by mechanical cleavage of graphite, preserves the predominant AB and ABC stacking of the graphene layers, while folding of FLG results in structures with layers, twisted with respect to the pure AB and ABC stacking. The twisted BLG (tBLG) and, more generally, twisted FLG (tFLG) allow for engineering of the electronic and optical properties, which can be a route for production of materials with desired physical properties for electronics and photonics.[2] The precise structural characterization of the synthesized tFLG samples is of paramount importance for future applications. This is normally performed by complementing theoretical and experimental methods. Among the latter, the Raman spectroscopy is an experimental techniques of choice because of its advantages of being a fast and non-destructive method.[3] The former ones are indispensable in supporting the assignment of the Raman spectra of the samples to definite structures.

The Raman spectra of tFLG exhibit an intense first-order Raman band, the so-called *G band*, originating from the in-plane Raman-active phonons, the so-called G phonons. Along with this band, a few other bands are also normally observed in the second-order Raman spectra of tFLG,[4,5] which come from two-phonon scattering processes and combined scattering by phonons and defects.[6] The second-order bands contain valuable information about the phonon dispersion, the electron–phonon and electron-photon couplings, doping, and strain in perfect structures, as well as on defects in imperfect ones.[7]

The Raman scattering by phonons in tFLG is found to be resonantly enhanced for certain laser excitation lines. The theoretical approach that properly describes the resonant character of the scattering is based on the quantum-mechanical perturbation theory with explicit account of the interactions between electrons, holes, photons, and phonons.[8] The direct calculation of the electronic and phonon dispersion and interaction matrix elements within the ab-initio approach is hindered by the huge computational efforts, required for the normally very large unit cells of tFLG. This problem can be mitigated by resorting to less rigorous models such as the tight-binding model, the most popular one being restricted to the use of one orbital per carbon atom and neglect of the orbitals overlap as well as limiting the calculations mainly to tBLG.[9] The parametrization[10] used in several publications[4,5,11] is limited to ppπ and ppσ intralayer and interlayer tight-binding parameters with neglect of the orbital overlap. These parameters are shown to perform satisfactorily for electronic transitions up to about 1 eV (Trambly de Laissardière *et al.*[10]) but are not shown to predict accurately enough the electronic dispersion for the whole range of the commonly used laser lines in Raman spectroscopy. In support of this conclusion, we note that the predicted optical conductivity is found to show significant deviation from the measured one.[12] The predicted first-order and second-order Raman bands *versus* laser excitation and twist angle correspond only semi-quantitatively to the available experimental data.[4] In the work of Sato *et al.*,[13] an extended tight-binding model, verified for optical properties of carbon nanotubes,[14] is used for the prediction of the G band of two tBLG.

Similarly to carbon nanotubes, it is often assumed that the Raman scattering by G phonons is enhanced for laser excitation equal to electronic transitions between states, contributing to symmetric spikes of the electronic density of states (eDOS).[4,14] Recent theoretical studies have shown that the enhancement takes place at laser excitations, larger than such electronic transitions.[5,11]

* *Correspondence to: Valentin N. Popov, Faculty of Physics, University of Sofia, Sofia 1164, Bulgaria.*
E-mail: vpopov@phys.uni-sofia.bg

Faculty of Physics, University of Sofia, Sofia 1164, Bulgaria

Along with this controversy about the resonance enhancement of the Raman bands, the existing calculations of the Raman bands of tBLG have the drawback of using insufficiently accurate models or are not performed systematically. Obviously, a systematic calculation of the G band for a variety of tBLGs within a realistic model will yield valuable results for practical use in the assignment of the absorption and Raman spectra to specific tBLG.

Here, we report a computational approach, based on a non-orthogonal tight-binding (NTB) model, for calculation of the eDOS, dielectric function, and REP of the G band of various tBLG. A perturbative scheme is employed for achieving a significant reduction of the computational time.

Theoretical

The crystal structure of tBLG can be considered as obtained by rotation of two AA-stacked graphene layers at an angle θ with respect to each other (Fig. 1, left). Rotations at angles θ and $\pm\theta$ modulo $\pi/3$ correspond to structures, which share the same electronic and phonon dispersion and, in this sense, can be considered as equivalent. Therefore, the properties of tBLG are unique within an interval that can be chosen as $0 \leq \theta \leq \pi/6$. Each tBLG can be characterized uniquely by the pair of integer numbers (p,q), $p \leq q$, (Shallcross *et al.*[15]) or (m,n), $m \leq n$, (Mele[16]) (here, the notation of Shallcross *et al.*[15] is used[17]), which determines the structural parameters, such as the unit cell, twist angle θ, and total number of carbon atoms 4 N in the unit cell. In particular, the AA-stacked BLG has $\theta = 0$ and (p,q) = (0,1), while the AB-stacked BLG has $\theta = \pi/3$ and (p,q) = (1,1). The determination of the structural parameters of a synthesized tBLG, based on experimental Raman data and calculated optical properties, is of significant practical interest.

Because of the resonant nature of the Raman scattering by tBLG, the proper theoretical approach is based on the quantum-mechanical perturbation theory and needs the knowledge of the electronic and phonon dispersions, and the matrix elements of the interactions between electrons and holes, photons, and phonons. The usually very large N poses a serious problem before the solving of the electron and phonon eigenvalue equations, because the straightforward approach needs computational time that increases rapidly with N. The subsequent modeling of the optical properties in third-order and higher-order perturbation theory is even much more demanding with respect to the computational resources.

The reduction of the complexity of the electron and phonon eigenvalue problem can be accomplished effectively by taking into account that the interlayer interaction is much weaker than the intralayer one and using the quantum-mechanical perturbation theory for degenerate electronic levels. The unperturbed electronic wavefunction of tBLG is chosen as a linear combination of the wavefunctions of the two isolated layers, each of them consisting of N two-atom unit cells, included in the unit cell of tBLG. The latter wavefunctions can be derived by solving N times the two-atom eigenvalue problem. The unperturbed wavefunction of tBLG can then be presented as a linear combination of the wavefuctions of all 2 N two-atom unit cells of the two isolated layers. The time for these calculations scales linearly with N. Next, the interlayer interaction Hamiltonian is considered as a perturbation. This Hamiltonian is represented as a sparse matrix, because of the short rangeness of the interactions, with number of elements, scaling linearly with N. The time for estimation of the elements of this matrix scales linearly with N. For deriving the corrected eigenstates, a small number r of unperturbed wavefunctions with eigenenergies in the energy window ±2 eV around the Fermi energy is considered. The calculation of the matrix elements of the interaction Hamiltonian between these wavefunctions is proportional to N times an r-dependent factor. Finally, the eigenvalue problem of rank r for lifting the degeneracy of the electronic levels is solved. Normally, r is much smaller than N and slightly increases with the increase of N. Therefore, the computational time for the electronic eigenvalue problem of tBLG increases quasilinearly with N.

Here, this perturbative approach to the calculation of the electronic, vibrational, and optical properties is applied in the framework of the NTB model, which has been proven to perform at a quantitative level for SLG[18,19] and BLG.[20,21] In particular, only matrix elements between the four atomic orbitals of type s, p_x, p_y, p_z for the valence electrons of the carbon atoms are considered.[20,22] The angular dependence of the matrix elements is described within the Slater–Koster scheme. The NTB model allows for the calculation of the total

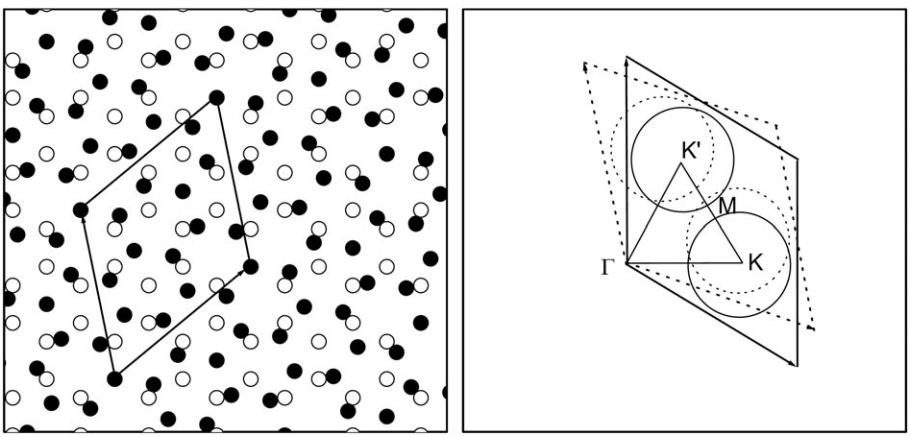

Figure 1. Left: unit cell of the smallest-period tBLG (1,3) ($\theta = 21.79°$, $N = 7$), drawn by solid lines. The atoms of the two layers are depicted by open and solid circles. Right: Brillouin zone of the two graphene layers of tBLG (1,3), shown by solid and dotted lines. The equi-energy cross-sections of the conic electronic bands (Dirac cones) are depicted schematically by solid and dotted circles. Upon twisting of one of the layers at an angle θ relative to the other, the Dirac cones of the layers no longer coincide but cross each other.

Journal of RAMAN SPECTROSCOPY

energy of the structure with important application for structural relaxation, which is a necessary step before performing calculations of the phonon dispersion. In particular, the atomic structure of the isolated layers is relaxed, after which, only the interlayer separation of the tBLG is relaxed. The relaxed interlayer separation for the studied tBLGs varies within 0.01 Å around the average value of 3.35 Å. Because such variation does not influence the presented results, the interlayer separation is fixed to the average one.

The NTB model underestimates the slope of the conduction and valence bands close to the Fermi energy, and the obtained electronic levels have to be multiplied by a factor of 1.18 for agreement with more sophisticated theoretical approaches and experiment.[4] This correction is taken into account everywhere later. The comparison of the approximate electronic eigenvalues with the exact ones for the AA-stacked and AB-stacked BLG revealed deviations within 10 meV.

The phonon dispersion of tBLG can also be derived within the NTB model. The obtained G phonons wavenumber differ from those for SLG by a few cm^{-1}. In view of the rather time-consuming calculations of the G phonons of tBLG and the smallness of the corrections to the phonon wavenumber, we adopt the G phonon of SLG with wavenumber of 1582 cm^{-1}.

The Raman intensity of the G band is calculated via an expression, derived in third-order quantum-mechanical perturbation theory.[18] The electron-photon and electron–phonon matrix elements, necessary for evaluating the perturbation series terms, as well as the energy-dependent electronic broadening parameter γ (half width at half maximum), are obtained within the NTB model. The calculations are limited to in-plane parallel scattering configuration, backscattering geometry, and Stokes processes. We note that the two-phonon Raman bands of tBLG can be calculated in a similar way but by means of fourth-order perturbation theory within the NTB model.

Results and discussion

Figure 2 shows the obtained electronic band structure, eDOS, imaginary part of the dielectric function ε_2, and REP of tBLG (1,3) ($\theta = 21.79°$, $N = 7$). Close to the Fermi energy, the conic electronic bands of the separate graphene layers, so-called Dirac cones, are rotated at an angle θ with respect to each other (Fig. 1, right). The interlayer interactions lift the degeneracy at the crossing of the bands in the vicinity of point M of the Brillouin zone (Fig. 1, right), and the linear electronic bands are deformed into parabolic ones close to the ΓM direction of the Brillouin zone (Fig. 2(a)). This modification of the bands has crucial effect on eDOS (Fig. 2(b)). In particular, bands 2 and 3 give rise to spikes, while bands 1 and 4 correspond to dips in eDOS. In analogy with carbon nanotubes, where the optical transitions take place between the symmetric spikes of eDOS, it is tempting to assume that this is the case here as well. However, transitions 1–4 and 2–3 are forbidden, while transitions 1–3 and 2–4 are allowed. Therefore, the transitions take place between corresponding pair of a spike and a dip of eDOS. This is verified by performing calculations of ε_2, taking into account all pairs of valence and conduction states with the same wavevector and broadening parameter of 1 meV. As clearly seen in Fig. 2(c), ε_2 exhibits a peak that corresponds to the mentioned allowed transitions. The position of this peak is the lowest *optical transition energy* E_{opt} of the tBLG. For the studied tBLG (1,3), E_{opt} is 3.61 eV, while the separation between the lowest pair of spikes in eDOS is lower and is equal to 3.27 eV. The REP of the G band (Fig. 2 (d)) is a broad band at the position of the allowed transitions. The characteristic asymmetric shape of the REP is due to the overlapping peaks for incoming resonance at E_{opt} and outgoing resonance at $E_{opt} + E_{ph}$, where $E_{ph} \approx 0.2$ eV is the energy of the G phonon. For laser excitations close to E_{opt}, the Raman signal is enhanced more than an order of magnitude relative to that from BLG with AB stacking.

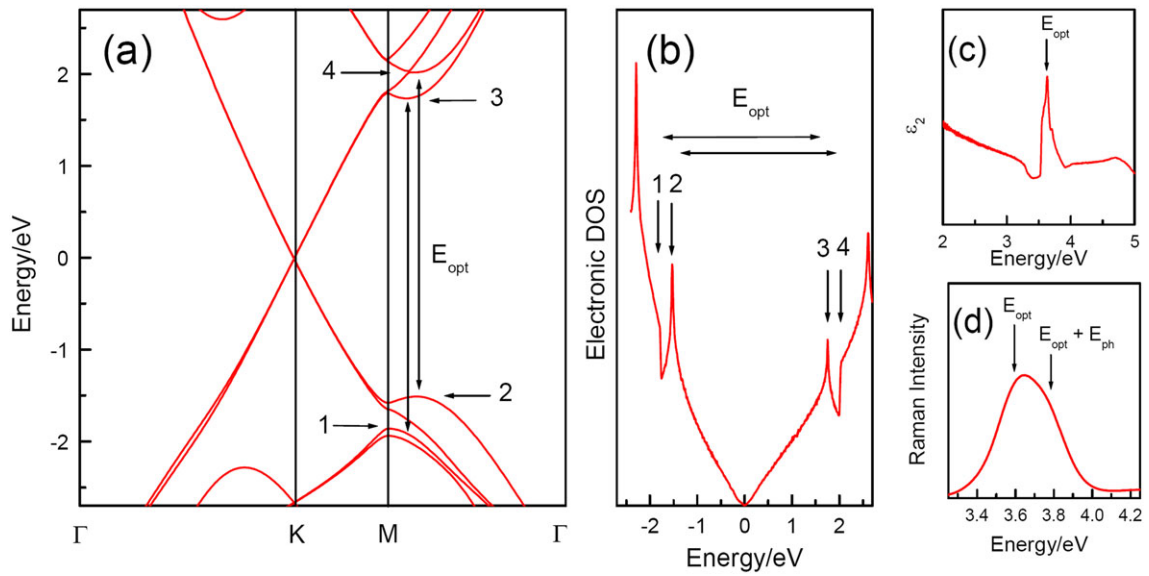

Figure 2. tBLG (1,3): (a) electronic band structure close to the Fermi energy along the principal directions in the Brillouin zone, (b) eDOS, (c) imaginary part of the dielectric function, and (d) REP of the G band. The numbers from 1 to 4 mark the extrema of the electronic bands with singularities of the eDOS along the ΓM direction of the Brillouin zone. The transitions between bands 1–3 and 2–4 are allowed and give rise to a peak of ε_2 at energy E_{opt} and a band in the Raman intensity, because of the overlapping incoming and outgoing resonances at energies E_{opt} and $E_{opt} + E_{ph}$ (E_{ph} is the energy of the G phonon).

In addition to the tBLGs (1,3) and (2,3), we calculate the electronic dispersion, eDOS, ε_2, and REP of the G band for the following tBLGs (p,q) [θ, N]: (1,5) [13.17°, 19], (1,7) [9.43°, 37], (5,7) [15.18°, 43], (1,4) [16.43°, 49], (1,9) [7.34°, 61], (7,9) [11.64°, 73], (4,5) [10.42°, 91], (1,6) [10.99°, 109], (5,6) [8.61°, 133], (11,13) [7.93°, 157], (1,8) [8.26°, 193], (11,15) [14.11°, 199], (2,9) [14.62°, 247], and (13,17) [12.36°, 259]. Except for (1,3), these are all 15 tBLGs with $7.3° < \theta < 17.9°$ and $N \leq 259$. The calculations can easily be extended to include tBLGs with even larger N.

The optical transition energies are derived from the peaks of ε_2 and are plotted as a function of θ in Fig. 3(a). It is seen that the mentioned range of θ corresponds to values of E_{opt}, which fall in the range of the common laser excitations for optical spectroscopy $1.3\ eV < E_L < 3.0\ eV$. More tBLGs can also be included in the calculations for θ outside the studied range of twist angles. Fitting a second-order polynomial to the points in Fig. 3(a), we derive the following dependence of E_{opt} (in eV) on θ (in deg):

$$E_{opt} = 0.19398\theta - 0.00135\theta^2 \quad (1)$$

Equation (1) can be used for derivation of E_{opt} for values of θ, known from structural studies, or for derivation of θ for E_{opt}, known from optical spectroscopy studies on a given tBLG sample. Apart from the dependence on θ, E_{opt} does not exhibit any obvious dependence on N and on the translation period of the unit cell. In the studied energy range and for the considered tBLG, no other optical transitions are present.

The comparison of the calculated E_{opt} with available experimental data exhibits deviations of up to 0.1 eV in the studied energy range (Fig. 3(a)). On the other hand, the values of E_{opt}, derived within the orthogonal tight-binding model,[11] systematically underestimate the experimental ones by about 0.2 to 0.6 eV in the same range. This observation shows clearly the advantages of our NTB model before the widely used one.[10]

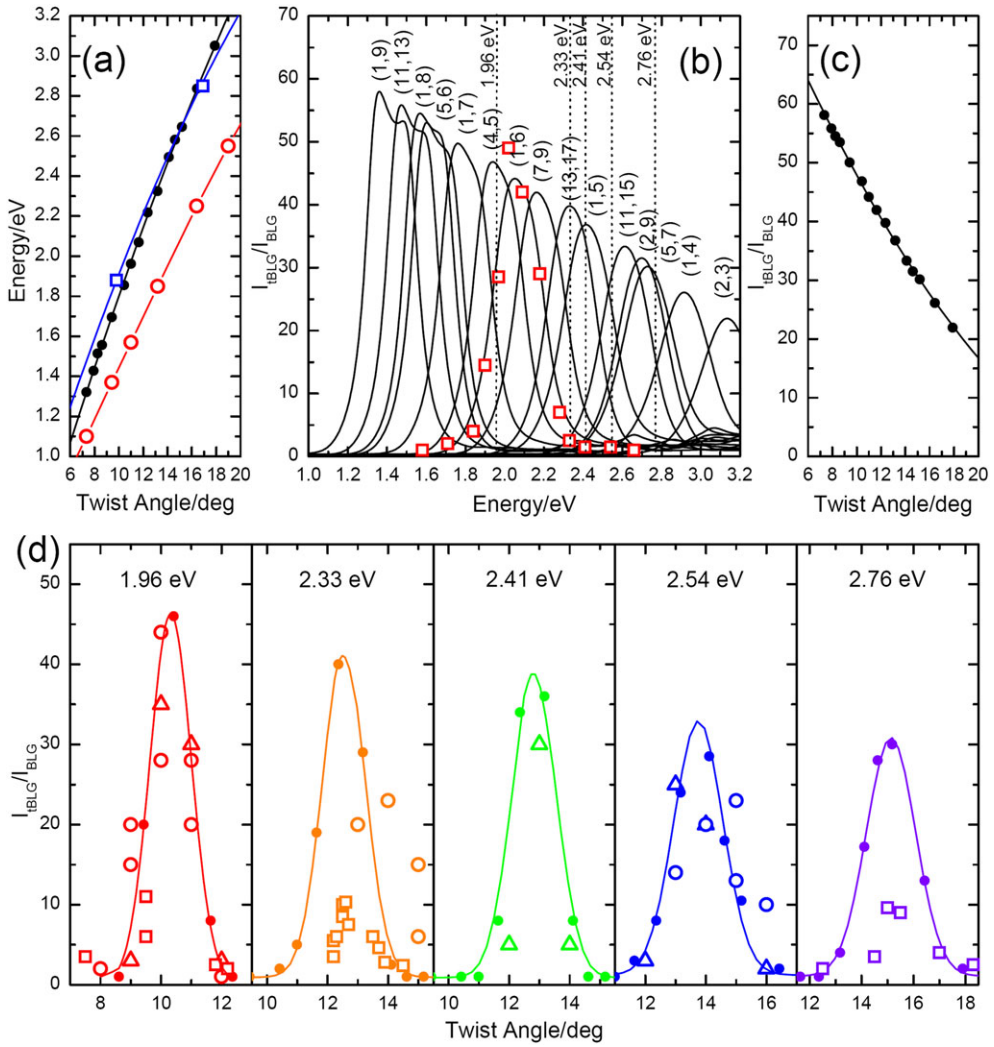

Figure 3. (a) E_{opt} vs θ, derived from the peaks of ε_2 (solid circles) and fitted with a second-order polynomial (line; see text) in comparison with available theoretical data[11] (empty circles; the line is a guide to the eye) and experimental data[12] (empty squares and a fitting line). (b) I_{tBLG}/I_{BLG} vs energy (REP) of selected tBLGs with indices (p,q). The vertical dotted lines are drawn at energies, which correspond to frequently used laser lines. The squares are experimental data for tBLG (4,5).[5] (c) Normalized peak intensity I_{tBLG}/I_{BLG} vs θ (solid circles), fitted with a second-order polynomial (line; see text). (d) I_{tBLG}/I_{BLG} vs θ (solid circles; the lines are guides to the eye) at five laser energies excitation lines. The solid circles are values at the crossings of the REPs and the dotted lines in panel (b). The experimental data are drawn with empty triangles,[25] empty squares,[24] and empty circles.[26]

Next, we perform calculation of the REP of the considered tBLGs. The electronic structure and all matrix elements are directly derived within the NTB model, while the estimation of γ is not so straightforward. In perfect graphene, both electron–phonon and electron–electron scattering processes contribute to γ but only the former contribution can be evaluated within the NTB model. Following the arguments that γ can be taken equal to twice the electron–phonon contribution,[23] we adopt for γ the energy-dependent expression[21]:

$$\gamma = 0.0252E + 0.0069E^2 \quad (2)$$

Here, γ and E are in eV. This expression gives excellent agreement of the predicted lineshape of the 2D band of AB-stacked BLG and the experimentally measured one.[21,23] For each tBLG, Eqn (1) is used in the expression for γ, Eqn (2), which is necessary for the calculation of the Raman intensity of the G band.

The derived intensity of the REP of the considered tBLGs, relative to that of BLG, $I_{norm} = I_{tBLG}/I_{BLG}$, is displayed in Fig. 3(b). At small energies, the REPs have two peaks, corresponding to the incoming and outgoing resonances, which are separated at the G phonons wavenumber. With increasing energy, the peaks are gradually smeared into a single peak. Because the width of the REP is determined by the G phonon wavenumber and the broadening parameter γ, the smearing of the two-peaked structure of REP with increasing energy can be attributed to the increase of γ with increasing E. The average half width at half maximum of the REPs of ~0.14 eV is in agreement with previous estimates.[5,13] The theoretical REP of tBLG (4,5) corresponds well to the observed one[5] apart from deviation of the peak value by a few per cent and the peak position by about 0.1 eV (Fig. 3(a)).

The peak value of I_{norm}, denoted as $I_{norm,peak}$, decreases monotonously with increasing θ (Fig. 3(c)). The second-order polynomial fit to these data is given by the following expression (θ is in deg)

$$I_{norm,peak} = 92.35 - 5.11\theta + 0.07\theta^2 \quad (3)$$

Finally, the calculated I_{norm} *versus* θ corresponds very well to the available experimental Raman data for a number of tBLG and five laser excitations[24–26] (Fig. 3(d)). However, while the agreement with experiment is excellent for E_L = 1.96 eV and very good for E_L = 2.41 eV, there are major deviations for E_L = 2.33, 2.54, and 2.76 eV. On the theoretical side, this discrepancy can be due to the uncertainty in the electron–electron contribution to γ. On the experimental side, it may be attributed to possible influence on the experimental I_{norm} by the substrate, doping, strain, and others, which is not accounted for in this study. Previous estimations[4] yield almost twice broader peaks of I_{norm} *versus* θ, which can be attributed to the used tight-binding parameters[10] and the large γ of about 0.2 eV. The very good agreement of our predictions with the available experimental data is a verification of the applicability of the proposed approach and the choice of γ for modelling the REP of the G band of tBLG.

Conclusions

We showed that the G band of tBLG can be modelled successfully at quantitative level using a perturbative technique within the NTB model. In particular, the origin of the resonance enhancement of the Raman signal is clarified, thus solving the existing controversy. The dependence of the optical transition energy on the twist angle is derived, the REP of the G band is calculated, and the dependence of the peak intensity of REP on the twist angle is derived. These predictions can be used for determination of the twist angle using the measured resonance energy of the G band in Raman experiments and, more generally, for support of the characterization of tBLG samples.

Acknowledgements

The author would like to acknowledge fruitful discussions with Ph. Lambin and L. Henrard.

References

[1] K. S. Novoselov, V. I. Fal'ko, L. Colombo, P. R. Gellert, M. G. Schwab, K. Kim, *Nature* **2012**, *490*, 192.
[2] F. Bonaccorso, Z. Sun, T. Hasan, A. C. Ferrari, *Nature Photonics* **2010**, *4*, 611.
[3] L. M. Malard, M. A. Pimenta, G. Dresselhaus, M. S. Dresselhaus, *Phys. Rep.* **2009**, *473*, 51.
[4] S. Coh, L. Z. Tan, S. G. Louie, M. L. Cohen, *Phys. Rev. B* **2013**, *88*, 165431.
[5] J.-B. Wu, X. Zhang, M. Ijäs, W.-P. Han, X.-F. Qiao, X.-L. Li, D.-S. Jiang, A. C. Ferrari, P.-H. Tan, *Nature Commun.* **2014**, *5*, 5309.
[6] C. Thomsen, S. Reich, *Phys. Rev. Lett.* **2000**, *85*, 5214.
[7] A. C. Ferrari, D. M. Basko, *Nat. Nanotechnol.* **2013**, *8*, 235.
[8] R. M. Martin, L. Falicov, in *Light Scattering In Solids. Topics of Applied Physics*, vol. 8 (Ed: M. Cardona), Springer, Berlin, **1975**, pp. 80–148.
[9] E. McCann, M. Koshino, *Rep. Prog. Phys.* **2013**, *76*, 056503.
[10] G. Trambly de Laissardière, D. Mayou, L. Magaud, *Nano Lett.* **2010**, *10*, 804.
[11] P. Moon, M. Koshino, *Phys. Rev. B* **2013**, *87*, 205404.
[12] R. W. Havener, Y. Liang, L. Brown, L. Yang, J. Park, *Nano Lett.* **2014**, *14*, 3353.
[13] K. Sato, R. Saito, C. Cong, T. Yu, M. S. Dresselhaus, *Phys. Rev. B* **2012**, *86*, 125414.
[14] M. S. Dresselhaus, A. Jorio, M. Hofmann, G. Dresselhaus, R. Saito, *Nano Lett.* **2010**, *10*, 751.
[15] S. Shallcross, S. Sharma, O. A. Pankratov, *Phys. Rev. Lett.* **2008**, *101*, 056803.
[16] E. J. Mele, *Phys. Rev. B* **2010**, *81*, 161405(R).
[17] The two notations are simply connected: m = (q – p)/k, n = (p + q)/k, where k is the greatest common divisor of p + 3q and 3q – x p. [15,16]
[18] V. N. Popov, P. Lambin, *Eur. Phys. J. B.* **2012**, *85*, 418.
[19] V. N. Popov, P. Lambin, *2D Materials* **2016**, *3*, 025014.
[20] V. N. Popov, C. Van Alsenoy, *Phys. Rev. B* **2014**, *90*, 245429.
[21] V. N. Popov, *Carbon* **2015**, *91*, 436.
[22] D. Porezag, T. Frauenheim, T. Köhler, G. Seifert, R. Kaschner, *Phys. Rev. B* **1995**, *51*, 12947.
[23] F. Herziger, M. Calandra, P. Gava, P. May, M. Lazzeri, F. Mauri, J. Maultzsch, *Phys. Rev. Lett.* **2014**, *113*, 187401.
[24] R. W. Havener, H. Zhuang, L. Brown, R. G. Hennig, J. Park, *Nano Lett.* **2012**, *12*, 3162.
[25] K. Kim, S. Coh, L. Z. Tan, W. Regan, J. M. Yuk, E. Chatterjee, M. F. Crommie, M. L. Cohen, S. G. Louie, A. Zettl, *Phys. Rev. Lett.* **2012**, *108*, 246103.
[26] H. B. Ribeiro, K. Sato, G. S. N. Eliel, E. A. T. de Souza, C.-C. Lu, P.-W. Chiu, R. Saito, M. A. Pimenta, *Carbon* **2015**, *90*, 138.